AFRL-ML-TY-TP-2005-4609

AN EXPERIMENTAL, NUMERICAL AND CFD INVESTIGATION INTO THE HEAT TRANSFER AND FLOW CHARACTERISTICS IN POROUS MEDIA USING A THERMAL NON-EQUILIBRIUM MODEL

Andrew M. Hayes, Aly H. Shaaban
Applied Research Associates, Inc, Tyndall AFB, FL 32403

Jamil A. Khan
University of South Carolina, Columbia SC

Ian G. Spearing
Liebert Corp, Columbus OH

Reza Salavani
Air Force Research Laboratory, Tyndall AFB, FL 32403

Interim Paper, October 2005

DISTRIBUTION STATEMENT A:

Approved for public release; distribution unlimited.

Air Force Research Laboratory
Materials and Manufacturing Directorate
Airbase Technologies Division
139 Barnes Drive, Suite 2
Tyndall AFB, FL 32403-5323

NOTICE

Using Government drawings, specifications, or other data included in this document for any purpose other than Government procurement does not in any way obligate the U.S. Government. The fact that the Government formulated or supplied the drawings, specifications, or other data does not license the holder or any other person or corporation; or convey any rights or permission to manufacture, use, or sell any patented invention that may relate to them.

This technical report was reviewed and cleared for public release by the Air Force Research Laboratory Tyndall Site (AFRL/MLQ) Public Affairs Office (PAO) and is releasable to the National Technical Information Service (NTIS). Reference PAO Case Number: AFRL/MLQ-06-045.

This report is releasable to the National Technical Information Service (NTIS) where it will be available to the general public, including foreign nationals.

5285 Port Royal Road
Springfield VA 22161
Telephone (703) 487-4650, (703) 487-4639 (TDD for the hearing impaired)
e-mail: orders@ntis.fedworld.gov
http://www.ntis.gov/index.html

This technical report is approved for publication.

/s/
REZA SALAVANI
Work Unit Manager

/s/
RICHARD N. VICKERS
Chief, Deployed Base Systems Branch

/s/
MICHAEL R. UPDIKE, Lt Col, USAF
Deputy Chief, Airbase Technologies Division

This report is published in the interest of scientific and technical information exchange and its publication does not constitute the Government's approval or disapproval of its ideas or findings.

REPORT DOCUMENTATION PAGE

Form Approved OMB No. 0704-0188

The public reporting burden for this collection of information is estimated to average 1 hour per response, including the time for reviewing instructions, searching existing data sources, gathering and maintaining the data needed, and completing and reviewing the collection of information. Send comments regarding this burden estimate or any other aspect of this collection of information, including suggestions for reducing the burden, to Department of Defense, Washington Headquarters Services, Directorate for Information Operations and Reports (0704-0188), 1215 Jefferson Davis Highway, Suite 1204, Arlington, VA 22202-4302. Respondents should be aware that notwithstanding any other provision of law, no person shall be subject to any penalty for failing to comply with a collection of information if it does not display a currently valid OMB control number.

PLEASE DO NOT RETURN YOUR FORM TO THE ABOVE ADDRESS.

1. REPORT DATE *(DD-MM-YYYY)*
01-10-2005

2. REPORT TYPE
Interim Technical Paper

3. DATES COVERED *(From - To)*
01-10-2003 -- 30-09-2005

4. TITLE AND SUBTITLE
An Experimental, Numerical, and CFD Investigation into the Heat Transfer and Flow Characteristics in Porous Media Using a Thermal Non-Equilibrium Model

5a. CONTRACT NUMBER
F08637-03-C-6006

5b. GRANT NUMBER

5c. PROGRAM ELEMENT NUMBER
62102F

5d. PROJECT NUMBER
4915

5e. TASK NUMBER
D1

5f. WORK UNIT NUMBER
4915D14D

6. AUTHOR(S)
Hayes, Andrew M.; Shaaban, Aly H.; Khan, Jamil A.; Spearing, Ian G.; Salavani, Reza

7. PERFORMING ORGANIZATION NAME(S) AND ADDRESS(ES)
Applied Research Associates, Inc.
P.O. Box 40128
Tyndall AFB, FL 32403

8. PERFORMING ORGANIZATION REPORT NUMBER

9. SPONSORING/MONITORING AGENCY NAME(S) AND ADDRESS(ES)
Air Force Research Laboratory
Materials and Manufacturing Directorate
139 Barnes Drive, Suite 2
Tyndall AFB, FL 32403-5323

10. SPONSOR/MONITOR'S ACRONYM(S)
AFRL/MLQD

11. SPONSOR/MONITOR'S REPORT NUMBER(S)
AFRL-ML-TY-TP-2005-4609

12. DISTRIBUTION/AVAILABILITY STATEMENT

Distribution Statement A: Approved for public release; distribution unlimited.

13. SUPPLEMENTARY NOTES

AFRL/MLQ Public Affairs Case # 06-049. Document contains color images.

14. ABSTRACT
Heat transfer and fluid flow through porous media was investigated using numerical simulations and experiment. For the numerical simulations, two models were created. The first consisted of a two-dimensional numerical model created in MathCAD and was solved using the finite difference approach. The MathCAD model's flow in the porous media was described by the Brinkman-Forchheimer-extended Darcy equation. The second model consisted of a computational fluid dynamics (CFD) porous media model using Fluent and was solved using the finite volume approach. Both models assumed constant fluid phase and properties. Pore diameters were held constant for each simulation; two different porosities were investigated. Boundary conditions were applied at the wall in which the temperatures of the fluid and the porous media were determined by coupled energy equations. The effects of the boundary condition, the Reynolds number, porosity, and heat input were examined.

15. SUBJECT TERMS

heat transfer, heat and mass transfer

16. SECURITY CLASSIFICATION OF: a. REPORT	b. ABSTRACT	c. THIS PAGE	17. LIMITATION OF ABSTRACT	18. NUMBER OF PAGES	19a. NAME OF RESPONSIBLE PERSON / 19b. TELEPHONE NUMBER *(Include area code)*
U	U	U	SAR	16	Reza Salavani / 850-283-3715

An Experimental, Numerical, and CFD Investigation into the Heat Transfer and Flow Characteristics in Porous Media Using a Thermal Non-Equilibrium Model

Andrew M. Hayes[1,2], Aly H. Shaaban[1], Jamil A. Khan[2], Ian G. Spearing[3], Reza Salavani[4]
[1]Applied Research Associates, Inc., Panama City, FL, USA
[2]University of South Carolina, Columbia, SC, USA
[3]Liebert Corporation, Columbus, OH, USA
[4]Air Force Research Laboratory, Tyndall AFB, Florida, USA

Abstract

Heat transfer and fluid flow through porous media was investigated using numerical simulations and experiment. For the numerical simulations, two models were created. The first consisted of a two-dimensional numerical model created in MathCAD and was solved using the finite difference approach. The MathCAD model's flow in the porous media was described by the Brinkman–Forchheimer-extended Darcy equation. The second model consisted of a computational fluid dynamics (CFD) porous media model using Fluent™ and was solved using the finite volume approach. Both models assumed constant fluid phase and properties. Pore diameters were held constant for each simulation; two different porosities were investigated. Boundary conditions were applied at the wall in which the temperatures of the fluid and the porous media were determined by coupled energy equations. The effects of the boundary condition, the Reynolds number, porosity, and heat input were examined.

The experimental investigation consisted of a flow channel with a porous media section that was heated from below by a heat source. The variation of temperature of the fluid in the porous media was measured along the centerline and along the top wall and bottom wall. The heat source temperature and the fluid's inlet and outlet temperatures were also measured. The results of the numerical and CFD models as compared to the experimental data for fluid flow through porous media are presented in the paper.

Nomenclature

F	inertia coefficient (dimensionless)
K	permeability $\left(m^2\right)$
P*	dimensionless pressure $\left(\dfrac{P}{\rho u_{in}^{2}}\right)$
u	velocity $\left(\dfrac{m}{s}\right)$
U	dimensionless velocity $\left(\dfrac{u}{u_{in}}\right)$
Vmag	velocity magnitude $\sqrt{u_x^{2}+u_y^{2}}$
Vol	volume $\left(m^3\right)$
X	dimensionless length $\left(\dfrac{L}{H}\right)$
Y	dimensionless height $\left(\dfrac{y}{H}\right)$
β	fluid-phase
ε	porosity
σ	solid-phase
λ	thermal conductivity $\left(\dfrac{W}{mK^{\circ}}\right)$
ϑ	dimensionless temperature $\dfrac{(T-T_{in})\lambda}{\dot{q}_w H}$

subscripts

D	darcian
d	dispersion
f	fiber
p	particle

v volumetric
x x-direction
y y-direction

1. Introduction

When fluid flows through a porous media such as a heat exchanger, packed bed regenerator, etc. the solution to the equations for fluid flow become difficult due to the tortuous geometry in which the fluid must navigate. In addition, the changes in porosity that flow can encounter add to the difficulty in obtaining a solution for the governing equations. Through the years many researchers have studied the flow characteristics and have added terms and laws to the equations in order to facilitate the conditions that the fluid sees as it flows through the porous media. Darcy's Law, the Brinkman extension and Forchheimer are typical additions. Also, when dealing with the heat transfer in the porous media, many researchers have derived boundary conditions for the model, such as local thermal equilibrium and local thermal non-equilibrium. Each of the two cases mentioned above require their own boundary conditions to be satisfied resulting in different solutions for the governing equations.

Over the last decade there has been an increased amount of research into the use of porous media as a heat transfer enhancement. Porous media heat exchangers (PMHE) offer a large amount heat transfer to occur within a small volume. Due to the large amount of surface area within the porous media, a PMHE can have a large volume to surface area ratio. As opposed to the local thermal equilibrium model (LTE), which assumes that the solid-phase temperature is the same at any point in the porous media, the local thermal non-equilibrium model (LTNE) assumes a finite difference between the fluid and the porous media and solves for their respective temperatures separately.

Numerous authors have studied the LTNE model's application to PMHE. Pavel *et al.* [2004] examined the influence different diameter porous media had on the Nusselt number. Their numerical code lacked accuracy due to the restrictions of the boundary conditions not applying to the physical model. Their conclusion was that porous media 0.8 times the inner diameter of the pipe offered the best enhancement of heat transfer while not significantly increasing the pressure drop. Alazmi and Vafai [2002], study how different boundary conditions can affect the heat transfer model. Different parameters such as the porosity, Darcy number, Reynolds number, inertia parameter, particle diameter, and solid-to-fluid conductivity ratio were analyzed. Jiang's *et al.* [2001] provided an in depth numerical model of heat transfer in a channel packed with various material. The numerical model's output is compared with experimental data for verification. The authors test various boundary conditions and settle on the ideal constant wall heat flux boundary condition, which describes the heat flux transferred by the fluid and by the solid phases are equal. Also discussed are the effects of viscous dissipation on the heat transfer coefficient, which was done using a numerical model. These and further considerations of thermal non-equilibrium as well as the thermal equilibrium models and other boundary conditions are outlined in Alazami and Vafai[2001], Jiang *et al.* [1999], Khashan and Al-Amiri[2005], Ochoa-Tapia and Whitaker[1997], Jeng *et al.* [2006], and Jen and Yan [2005].

2. Numerical, CFD and Laboratory Models

Heat transfer and flow through porous media was modelled with MathCAD and Fluent™. The effects of the boundary condition, the Reynolds number, heat input, and porosity were all examined. The numerical model assumed constant fluid phase, constant pore diameter per porosity experiment, viscous dissipation, no conduction in the *x-direction* through the porous media, and thermal non-equilibrium in which the temperature of the fluid and the porous media are at different temperatures. The numerical model was two-dimensional and solved using the finite difference approach. The momentum equations were solved first to obtain the velocity profiles. These velocity profiles were then used in the energy equation to solve for the heat transfer characteristics of the fluid and the porous media.

The Fluent™ model was based on flow through porous media and solved using the finite volume method. The Fluent™ model had a constant heat flux applied to one side of the porous media with fluid travelling through the porous media. The permeability and inertia coefficient were defined along with other fluid characteristics within the Fluent™ model.

The experimental set-up, similar to Boomsma and Poulikakos [2001] and Jiang *et al.* [2001], consisted of a flow channel with a porous media section that was heated from below. The temperatures of the fluid in the porous media were measured down the centerline and along each of the walls. The heater block temperature was also monitored, as well as the fluid's inlet and outlet temperatures. The pressure drop was measured across the porous media section in order to determine the variables used in Fluent™ and the numerical model. Finally, the results of the numerical and Fluent™ models were compared to the experimental data.

3. Numerical Two-Dimensional Flow Model for Porous Media

The steady-state two-dimensional governing equations for single phase fluid flow in an isotropic, homogenous, porous media based on the Brinkman-Darcy-Forchheimer model with constant properties has been presented by numerous authors and can be written as;

$$\frac{\rho_f}{\varepsilon^2}(u \bullet \nabla)u = -\nabla P - \frac{\mu}{K}u + \frac{F\rho_f}{\sqrt{K}}|Vmag|u + \frac{\mu}{\varepsilon}\nabla^2 u \tag{1}$$

Equation (1) was separated into x and *y-direction* components and represented non-dimensionally as;

For the *x-direction*;

$$U_x\frac{\partial U_x}{\partial X} + U_y\frac{\partial U_x}{\partial Y} = -\varepsilon\frac{\partial P^*}{\partial X} - \frac{\varepsilon^2}{\mathrm{Re}\,Da}U_x + \frac{F\varepsilon^2}{\sqrt{Da}}|Umag|U_x + \frac{\varepsilon}{\mathrm{Re}}\left(\frac{\partial^2 U_x}{\partial X^2} + \frac{\partial^2 U_x}{\partial Y^2}\right) \tag{2}$$

And the *y-direction*

$$U_x\frac{\partial U_y}{\partial X} + u_y\frac{\partial U_y}{\partial Y} = -\varepsilon\frac{\partial P^*}{\partial Y} - \frac{\varepsilon^2}{\mathrm{Re}\,Da}U_y + \frac{F\varepsilon^2}{\sqrt{Da}}|Umag|U_y + \frac{\varepsilon}{\mathrm{Re}}\left(\frac{\partial^2 U_y}{\partial X^2} + \frac{\partial^2 U_y}{\partial Y^2}\right) \tag{3}$$

Taking the curl and using the definition of the velocity in terms of the stream-function yields;

$$\frac{\varepsilon}{Da}\left(\nabla^2\psi\right) + \nabla^4\psi = \frac{\mathrm{Re}}{\varepsilon}U_x\left[\left(\frac{\partial^3\psi}{\partial x^3}\right) + \left(\frac{\partial^3\psi}{\partial y^2\partial x}\right)\right] + \frac{\mathrm{Re}}{\varepsilon}U_y\left[\left(\frac{\partial^3\psi}{\partial x^2\partial y}\right) + \left(\frac{\partial^3\psi}{\partial y^3}\right)\right] \tag{4}$$

Equation (4) represents the stream function-velocity model for flow through porous media. Equation (4) was solved by an iterative approach, as presented by Gupta et al. [2005].

In order to solve equation (4) it was necessary to obtain the permeability and inertia coefficients. The Forcheimer equation was used to obtain these values

$$\Delta p = \frac{\mu L}{K}u_D + \frac{\rho F L}{\sqrt{K}}u_D^2 \tag{5}$$

By substituting in $C_1 = \frac{\mu L}{K}$ and $C_2 = \frac{\rho F L}{\sqrt{K}}$ equation (1) can be rewritten as:

$$\Delta p = C_1 u_D + C_2 {u_D}^2 \tag{6}$$

Then, by obtaining the pressure drop at different Darcian velocities across the porous media and plotting the results the coefficients; C_1 and C_2 were determined by a second order polynomial curve fit. From knowing the coefficients it was possible to obtain the permeability, K and the inertia coefficient, F.

These values of the permeability and the inertia coefficient were used in the numerical model as well as the Fluent™ models.
After knowing the permeability the Darcy, *Da,* number could be found for the porous media flow;

$$Da = \frac{K}{H^2}$$

4. Numerical 2-D Heat Transfer Model

The fluid-phase and solid-phase energy equations for the thermal non-equilibrium model with consideration of thermal dispersion, viscous dissipation, constant porosity and constant properties, and neglecting conduction in the porous media in the *x-direction* due to the high Peclet number flows being investigated $(118 < Pe < 416)$, were as follows; for the fluid phase;

$$\rho_f Cp_f \varepsilon \left[u_x \frac{\partial (T_f)}{\partial x} + u_y \frac{\partial (T_f)}{\partial y} \right] =$$

$$\frac{\partial}{\partial y}\left(\varepsilon \lambda_f + \lambda_d\right)\left[\frac{\partial T_f}{\partial y}\right] + \frac{\varepsilon \mu_f}{K} u_x^2 + \varepsilon^2 \frac{\rho_f F}{\sqrt{K}} |Vmag| u_x^2 + \frac{h_v}{\varepsilon}(T_s - T_f) \qquad (7)$$

And for the solid phase;

$$(1-\varepsilon)\frac{\partial}{\partial y}\left[\lambda_s \frac{\partial T_s}{\partial y}\right] - \frac{h_v}{\varepsilon}(T_s - T_f) = 0 \qquad (8)$$

Non-dimensionalizing (7) yielded;

$$U_x \frac{\partial (\theta_f)}{\partial X} + U_y \frac{\partial (\theta_f)}{\partial Y} = \frac{1}{\varepsilon \operatorname{Re} \operatorname{Pr}}\left[\frac{\partial}{\partial Y}\left(\frac{\varepsilon \lambda_f + \lambda_d}{\lambda_f}\right)\frac{\partial \theta_f}{\partial Y}\right]$$

$$+ \frac{1}{Da \operatorname{Re}} \frac{u_{in}^2 \varepsilon \lambda_f}{Cp_f \dot{q}_w H}\left(U_x^{\,2}\right) + \frac{u_{in}^2 F \varepsilon^2 \lambda_f}{Cp_f \dot{q}_w H \sqrt{Da}} |Umag| U_x^{\,2} + \frac{Nu_{sf}}{\operatorname{Re} \operatorname{Pr}}\left[\frac{\partial^2 \theta}{\partial Y^2}\right] \qquad (9)$$

And (8) yielded;

$$(1-\varepsilon)\frac{\lambda_s}{\lambda_f}\left[\frac{\partial^2 \vartheta_s}{\partial Y^2}\right] - Nu_{sf}(\vartheta_s - \vartheta_f) = 0 \qquad (10)$$

The equations were descretized and then solved using the implicit finite difference method and using the velocities found by the two-dimensional stream function-velocity model equation (4).
The boundary condition at the heated wall for the thermal non-equilibrium model was the same as mentioned by Jiang *et al.*[2001].

$$\dot{q}_w = -\lambda_{fw}\left(\frac{\partial T_f}{\partial y}\right)_w = -\lambda_s\left(\frac{\partial T_s}{\partial y}\right)_w \qquad (11)$$

With

$$h_v = 6 h_{sf} \frac{(1-\varepsilon)}{d_p} \qquad (12)$$

The Reynolds number could be represented by the following correlations Jiang *et al.*[2004], Alazmi and Vafai [2001], and Boomsma and Poulikakos [2001].

$$\operatorname{Re} = \frac{\rho u_D d_f}{\mu}, \operatorname{Re} = \frac{\varepsilon \rho u_D d_p}{\mu}, \operatorname{Re} = \frac{u_{in} D_h}{\nu \varepsilon}, \operatorname{Re}_h = \frac{\operatorname{Re}}{(1-\varepsilon)}, \operatorname{Re} = \frac{\rho u_D \sqrt{K}}{\mu}$$

The equation for the Reynolds number was used in this research, unless otherwise noted, was

$$\operatorname{Re} = \frac{2 M d_p}{3\mu(1-\varepsilon)} \qquad (13)$$

The local heat transfer coefficient was calculated as;

$$h_x = \frac{\dot{q}_w}{(T_{wx} - T_{fm})} \tag{14}$$

The local temperature of the heat transfer surface was calculated using the measured temperatures of the wall.

$$T_{wx} = T_x - \frac{\dot{q}_w \delta}{\lambda_s} \tag{15}$$

Other equations for the Nusselt number were

$$Nu_{sf} = h_{sf} d_p \lambda_f = \left[\left(1.18\,\mathrm{Re}^{.58}\right)^4 + \left(0.23\,\mathrm{Re}_h^{0.75}\right)^4 \right]^{.25} \tag{16}$$

And also;

$$\frac{1}{h_{sf}} = \frac{d_p}{Nu_{sf}\,\lambda_f} + \frac{d_p}{\beta \lambda_s} \quad , \quad Nu_{sf} = \frac{0.255}{\varepsilon} \mathrm{Pr}^{.33}\,\mathrm{Re}^{.66}, \quad \beta = 10$$

Jiang *et al.*[1999] presented a modified thermal dispersion equation;

$$\lambda_d = C(\rho Cp)_f\, d_p \sqrt{u_{x_p}^{\ 2} + u_{y_p}^{\ 2}}\,(1-\varepsilon) \tag{17}$$

With

$$C = 1.042\left(\rho_f Cp_f\, d_p u_p (1-\varepsilon_m)\right)_0^{-.8282} \tag{18}$$

And

$$D_h = \frac{2hW}{(h+W)} \tag{19}$$

The equations were used along with the data obtained from the laboratory experiments to model the heat transfer in porous media. These results were then compared to the output from the Fluent™ model and from the numerical model.

5. Fluent™ Model

The porous media model in fluent was a two-dimensional model consisting of a flow channel with a mid-section representing the porous media. Gambit was used to create the geometry and the mesh of the model. The mesh was finer at the entrance and exit of the porous media. The grid spacing for the porous media was decreased in order to increase the accuracy of the calculation used to determine the flow characteristics and heat transfer within the porous media.

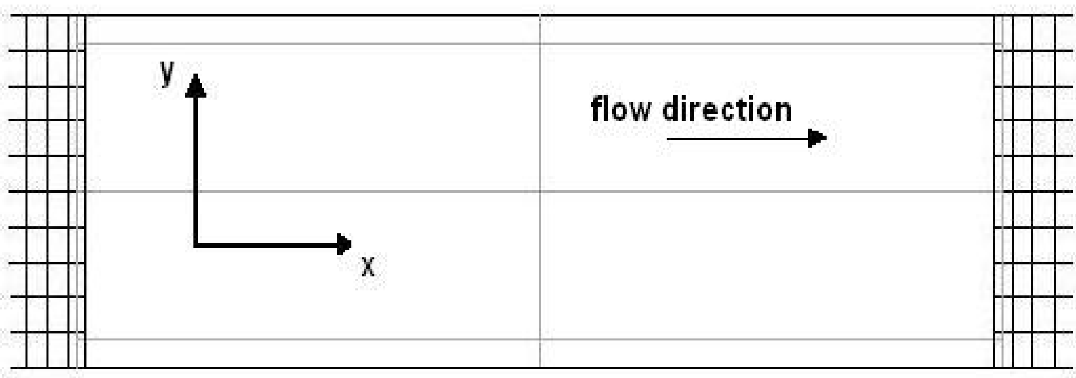

Figure 1. Temperature Plane Representation in the Porous Media Model

The dimensions of the Fluent™ model matched the dimensions of the physical model used in the laboratory experiments. Figure 1 shows the planes used to record temperature data within the porous media. The planes are grey in color. They are in both the *x* and *y-direction* and are located at the entrance, exit, top, bottom, horizontally through the middle as well as vertically through the

middle. The horizontal planes represent the location of the thermocouples used in the laboratory experiment. The flow in Figure 1 was from left to right.
Fluent™'s porous media model contained settings for the following variables; the viscous resistance, the inertia resistance, and the porosity. The viscous resistance and the inertia resistance values were obtained from the experiment.

The boundary condition used by Fluent™ for the heat flux was;

$$\dot{q} = h_f \left(T_s - T_f\right) \tag{20}$$

Whereas, the fluid side heat transfer was calculated using

$$\dot{q}_w = -\lambda_f \left(\frac{\partial T}{\partial y}\right)_w \tag{21}$$

For post processing Fluent™ was used as well. The post processing involved the output files of velocity in the *x* and *y-direction*, the heat input, and the temperatures. Each of the laboratory experiments were replicated in Fluent™. The data was collected and graphed for comparison.

6. Experimental Apparatus and Data Collection

The physical model used in the experiments was very similar to the model used by Jiang *et al.* [2001]. The model assumes the porous media was isotropic and homogeneous; the fluid was single phase, constant porosity, and constant properties. The lower side of the porous media received a constant heat flux, while the upper side was adiabatic. The test apparatus is shown in Figure 2. The fluid channel dimensions were .0381m x .0381m x .0127m. The size of the heated test section was .038m x .038m. The heater block in the lower plate of the channel received a constant heat flux, $\dot{q}_w$. The flow entered the channel with an average velocity, u_{in}, and constant temperature, T_{in}.

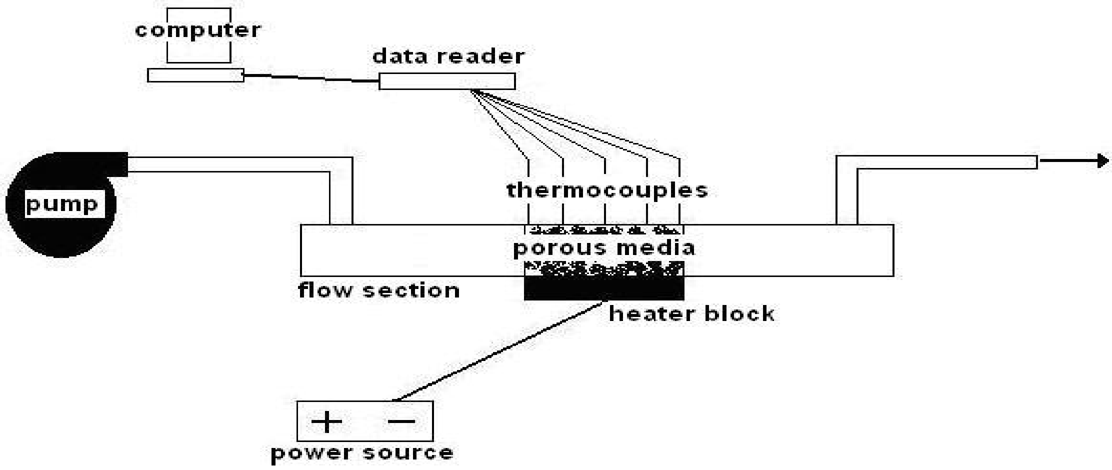

Figure 2. Experimental Apparatus

The test section was made from lexan, and consisted of an upper and lower section. The lower section contained the flow channel and section for the porous media. The porous media was obtained from ERG Aerospace, Inc. constructed of aluminum 6101 with constant porosities. Two different pore sizes were tested; 10PPI (pores per inch) and 40PPI. The upper section also contained the inlet and outlet holes for the fluid as well as the thermocouple insertion points. The lower section contained the heat block constructed of 38mm x 38mm x 19mm thick aluminum which held two 120V/20W heaters 6.35mm diameter and 25.4mm length.

Equally spaced thermocouples were inserted mid-way into the porous media along the horizontal center line of the test section, along the wall at the top corner, and along the bottom corner in order to monitor the fluid's temperature at each of the locations. The heater block's temperature was also monitored with a thermocouple. The inlet and outlet temperature of the fluid was measured with a thermocouple placed at the inlet region and exit region of the lexan test apparatus. Inlet pressure was monitored using a pressure transducer. The mass flow rate of the water was controlled by 3-piston pump. For each experiment, water was used as the working fluid, passing it through the porous media while holding fixed the flow rate, inlet temperature, and heat power, and recording results at steady state when the outlet temperature of the water did not fluctuate more than ± .02 degrees Celsius. Successive experiments changed heater power, then the procedure was repeated for the second porous sample.

In order to determine the heat loss from the heat section to the adjacent section by conduction, to the atmosphere by radiation and convection a separate experiment was preformed very similar to Pavel [2004].

6. Fluent™ Porous Media Results

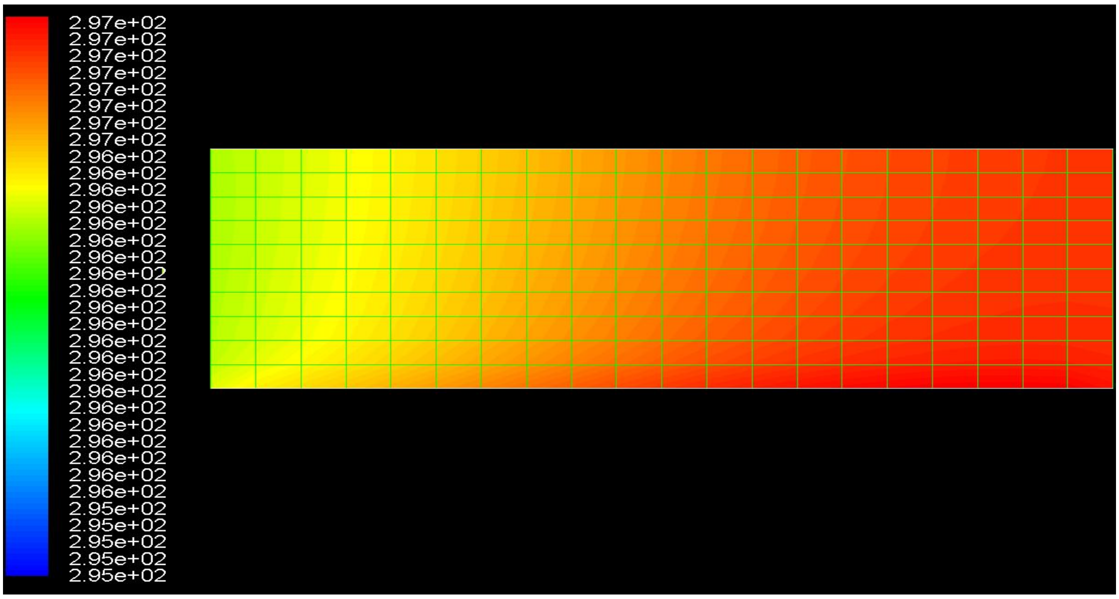

Figure 3. Fluent™ Fully Developed Fluid Temperature Profile for Steady-State Porous Media Flow

After determining the inertia and viscous terms it was possible to set the boundary conditions in Fluent™. Typical results for the fluid temperature within the porous media are presented in Figure 3. Since the heat was applied only at the bottom wall, the temperature of the fluid was at the highest at the bottom of the porous media and increased as the fluid traveled in the x-*direction* along the same plane. The temperature in *y-direction* along the same plane decreased as the distance from the bottom wall increased. The Fluent™ model was used to represent the one-equation (LTE) model.

7. Two-Dimensional Numerical Fluid Flow Results

As opposed to the typical parabola velocity profile that is typical of flow between pipes, the addition of the resistance terms to the momentum equation that treats the porous media as a pressure jump resulted in steep velocity gradients near the wall, and a more uniform velocity profile within the porous media region.

8. Laboratory Results

The laboratory experiment mentioned earlier resulted in the temperature profiles for different Reynolds numbers, different heat inputs, and different porosities. The results below will compare the local heat transfer coefficient with numerical data based on the fluid temperature next to the wall. The heat transfer coefficient based on the mean fluid temperature will also be discussed; both will be compared to the data obtained from Fluent™ data. The thermal dispersion of the different porosities will be discussed. The porous media pieces were made from aluminum with the thermal conductivity of $170\frac{W}{mK}$. The fibre diameter of the coarse porosity piece was $.004m$, while the diameter of the finer porosity piece was $.001m$. The dimensions of the porous media were $0381m$ x $.0381m$ x $.0127m$. The fine porous media had a porosity of .925, while the coarse porous media had a porosity of .9167. Velocities ranging from $.0006\frac{m}{s}$ to $.002\frac{m}{s}$ were used to evaluate the heat transfer capabilities. These velocities resulted in values of $.6 \le \mathrm{Re} \le 3$ for the fine media, and $.8 \le \mathrm{Re} \le 3.2$ for the coarse media. The temperature profiles of the recorded data showed the temperatures rising as the fluid moved along the *x-direction* through the porous media through the interaction with the heated porous media. The maximum temperatures were recorded at the bottom of the porous media due to the heat input being at the bottom. The temperatures decreased the further the fluid was from the heat source.

The friction factor for the flow in the fine porosity was based on Jiang *et al.* [1999];

$$f = \frac{\varepsilon_m^3}{1-\varepsilon_m}\frac{\rho_f d_p}{3M^2}\frac{\Delta P}{L} \qquad (22)$$

Where, the mass flux, M, is $M = \rho_f u$ and $\varepsilon_m = \frac{Vol_t - Vol_p}{Vol_t}$.

Jiang et al. [1999] also presented a correlation for the friction factor as a function of Reynolds number

$$f = \frac{36.4}{\mathrm{Re}} + .45 \qquad (23)$$

This value is valid for Re_e<2000. It was found that the experimental data correlated well with equation 23.

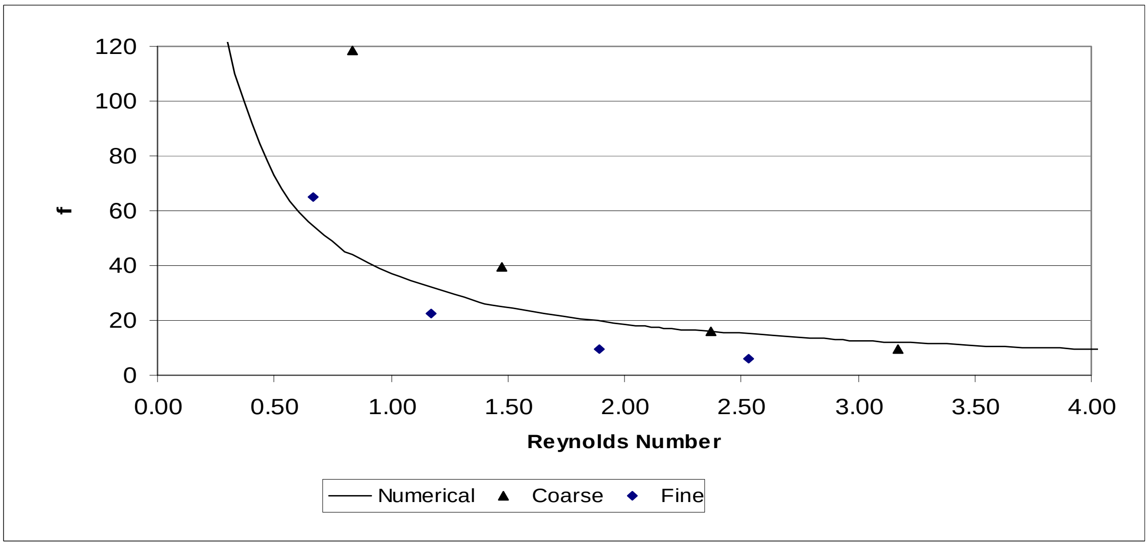

Figure 4. Friction Factor Based on Reynolds Number

The heat transfer coefficient was found using the entrance temperature of the fluid as recorded by thermocouple. The results can be seen in the figures below. As mentioned by other authors, the entrance effects were hard to capture with the laboratory experiment. The Fluent™ line represents the average of the results of the different Reynolds numbers for specific heat input. Typical graphs are represented below. The graphs show that the heat transfer coefficient was at a maximum in the beginning of the flow channel. This was due to the mixing that was occurring at the entrance of the porous media. The numerical model captured this well, while the laboratory model was not as accurate. The Fluent™ model over predicted the heat transfer coefficient.

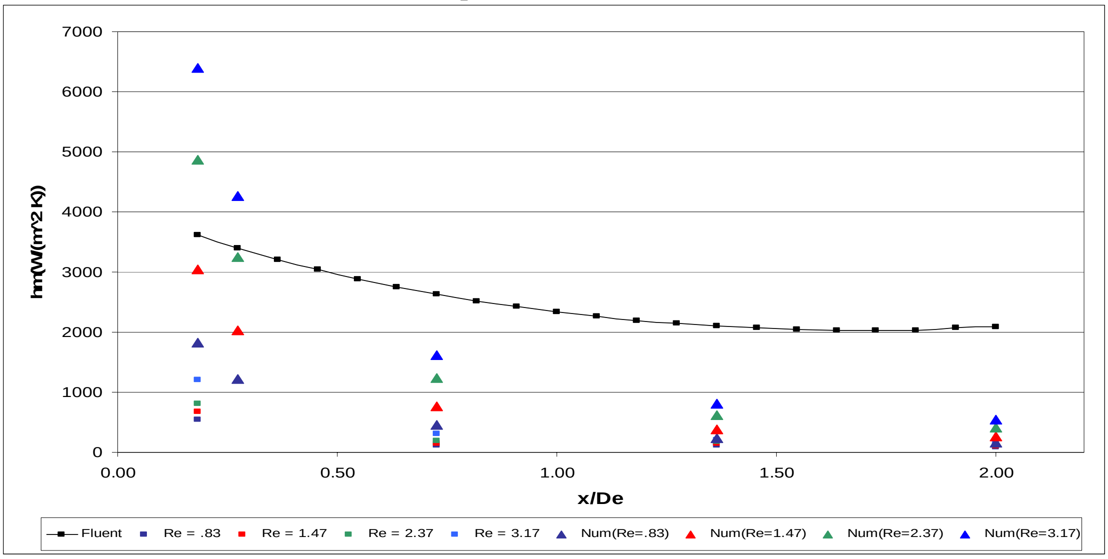

Figure 5. Heat Transfer Coefficient Based on Entrance Fluid Temperature at 1.64kW/m^2 Coarse Media

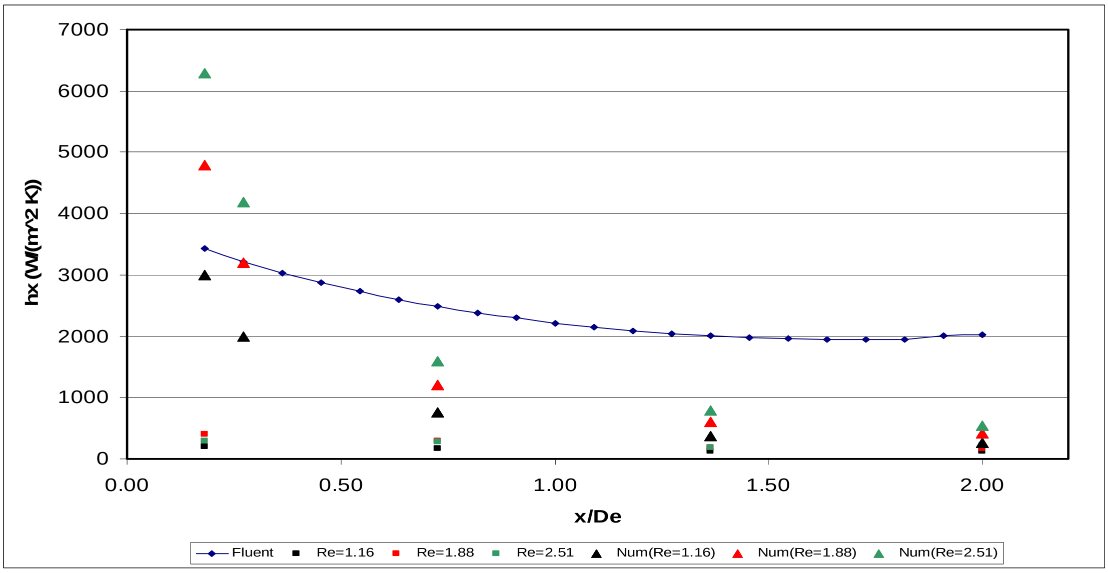

Figure 6. Heat Transfer Coefficient Based on Entrance Fluid Temperature at 1.0kW/m^2 Fine Media

The amount of surface area in porous media was large; therefore the amount of water in contact with the porous surface was also large. The amount of heat transfer credited to the thermal dispersion given in equation (17) increased as the Reynolds number increased. The thermal dispersion for each of the Reynolds number is plotted below. From the graph it can be seen that the amount of heat transfer due to thermal dispersion is small at the low Reynolds number. Therefore, it can be neglected.

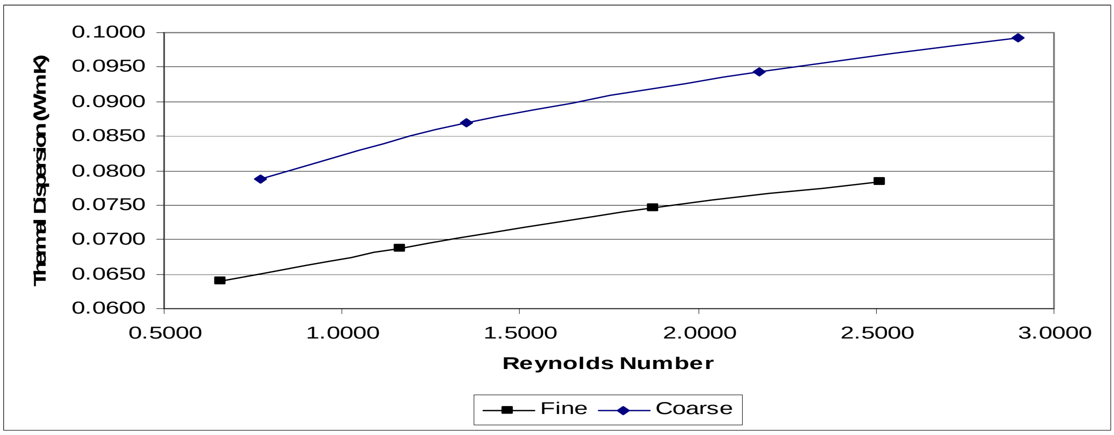

Figure 7. Thermal Dispersion as a Function of Reynolds Number

9. Verification of the Local Thermal Non-Equilibrium Model

In order to validate the use of the LTNE model different approaches were used to quantify the resulting data. Whitaker [1999] proposed methods for the validation of the use of the two-equation model based on the volume averaging technique.

In order to validate the use of only the one-equation model Whitaker proposed, through rigorous mathematical modelling, that if certain conditions were met the use of a one-equation model was valid.

Whitaker's restrictions to use of the thermal equilibrium model were as follows:

1. Either ε_β or ε_σ tends to zero.
2. The difference in the β-phase and σ-phase physical properties tends to zero.
3. The square of the ratio of length scales, $\left(\frac{l_{\beta\sigma}}{L}\right)^2$, tends to zero.

The porous media, when subjected to the above criterion, must be modelled with the two equation model. Criteria 1 was not satisfied because the porosity of the two phases in the porous media did not tend to zero. Criteria 2 was not satisfied because the difference physical properties of water and aluminum did not tend to zero. Finally, Criteria 3 was not satisfied because the quotient of the length between the phases and the length of the system in which the phases were evaluated did not tend to zero.

Another method for determining whether or not the thermal equilibrium model was valid was set forth by Jeng [2005]. Jeng introduced an operator, Ω, that was a function of the ratio of the volumetric heat transfer, h_v, and the effective thermal conductivity of the solid, λ_{seff}.

This was derived from the division of the flow path of the heat from the heated surface to the fluid stream into two channels; the first being from the heated wall to the fluid, and the second being the indirect method through the solid matrix to the fluid. Also, realizing that the thermal condition between the fluid and the solid matrix will be closer to thermal equilibrium when the fin efficiency was smaller a relationship between the volumetric heat transfer and the thermal conductivities of the fluid and solid could be developed;

$$\eta h_v H^* \le h_v \frac{h_v}{\lambda_{seff} + \lambda_{feff} + \lambda_d} \tag{24}$$

Using other relationships presented in the paper, Jeng's final equation was as follows:

$$\Omega = \left(\sqrt{\frac{h_v}{\lambda_{seff}}} H^*\right) \tanh\left(\sqrt{\frac{h_v}{\lambda_{seff}}} H^*\right) \tag{25}$$

In order to satisfy the conditions of local thermal equilibrium it was necessary for $\Omega > 3$. For all other conditions the two-equation model could be used. When the equation was applied to the data

obtained from the laboratory experiments and the numerical simulation the value of Ω was below three.
And, finally, another method to ensure the use of the two-equation model was based on Kashan's [2004] definition that stated;
In essence, the LTNE condition is declared when the criterion $\left|\vartheta_s - \vartheta_f\right| \geq .05$ *is satisfied at any computational node inside the tube domain including the developing region.*
The LTNE condition was checked at each of the Reynolds numbers and heat input experiments. A typical output showing the difference is below. As can be seen, the value of .05 is present in the computational domain. Therefore, the local thermal non-equilibrium model was the correct model to use.

Furthermore, by investigating the figures above in which the Fluent™ model (LTE) was included it can be seen that the one-equation model did not match the data to an extent that warranted its use in the thermal modelling of porous media. The numerical data and the laboratory data matched up well, which further justified the use of the two equation model.

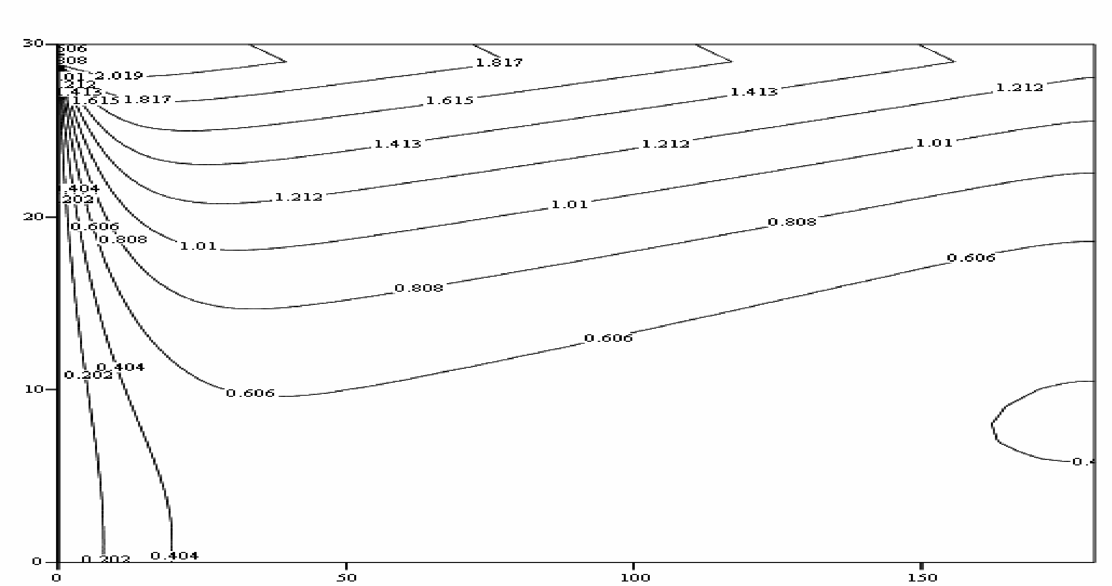

Figure 8. Dimensionless Temperature Difference Between Solid and Fluid in Porous Media

10. Conclusions

A thermal non-equilibrium model was developed to investigate the heat transfer in porous media. It was compared to the data obtained from a laboratory experiment and to the data of a Fluent™ model. The results of the numerical model compared well with the laboratory experiments, while the Fluent™ model, using the thermal equilibrium equation, over predicted the heat transfer. The criteria set forth by other authors were also used to validate the thermal non-equilibrium model's usage when modelling the heat transfer in porous media.

REFERENCES

1. Alazmi, B., Vafai, K., *Constant Wall Heat Flux Boundary Conditions in Porous Media Under Local Thermal Non-equilibrium Conditions*, International Journal of Heat and Mass Transfer, **45**, 2002, 3071-3087.
2. Alazmi, B., Vafai, K., *Analysis of Fluid Flow and Heat Transfer Interfacial Conditions Between a Porous Medium and a Fluid Layer*, International Journal of Heat and Mass Transfer, **44**, 2001, 1735-1749.
3. Boosma, K., Poulikakos, D., *On the Effective Thermal Conductivity of a Three-Dimensionally Structured Fluid-Saturated Metal Foam*, International Journal of Heat and Mass Transfer, **44**, 2001, 827-836.

4. Boosma, K., Poulikakos, D., Zwick, F, *Metal Foams as Compact High Performance Heat Exchangers*, Mechanics of Materials, **35**, 2003, 1161-1176.
5. Burmeister, Louis C., *Convective Heat Transfer*, 2nd Edition, John Wiley & Sons, Inc., New York, 1993.
6. ERG Materials and Aerospace Corporation, 900 Stanford Avenue, Oakland, CA 94608, Phone (510)-658-9785, Fax (510)-658-7428.
7. Fluent, Inc. 10 Cavendish Court, Centerra Park Lebanon, New Hampshire 03766 Phone: (603) 643-2600 Fax: (603) 643-3967.
8. Ghia, U., Ghia, K. N., Shin, C.T., *High Re Solutions for Incompressible Flow Using the Navier Stokes Equations and a Multigrid Method*, Journal of Computational Physics, **48**, 1982, 387-411.
9. Gupta, Murli M., Kalita, Jiten C., *A New Paradigm for Solving Navier-Stokes Equations: Streamfunction-Vorticity Formulation*, Journal of Computational Physics, **207**, 2005, 52-68.
10. Howes, Frederick A., Whitaker, Stephen, *The Spatial Average Theorem Revisited*, Chemical Engineering Science, Vol. 40, No. 8, 1995, 1387-1392.
11. Incropera, F.P., DeWitt, D.P., *Fundamentals of Heat and Mass Transfer*, 3rd Edition, John Wiley & Sons, Inc., New York, 1990.
12. Jiang, Pei-Xue, Wang, Zhan, Ren, Ze-Pei, Wang, Bu-Xuan, *Experimental Research of Fluid Flow and Convection Heat Transfer in Plate Channels Filled With Glass or Metallic Particles*, Experimental Thermal and Fluid Science, **20**, 1999, 45-54.
13. Jiang, Pei-Xue, Ren, Ze-Pei, *Numerical Investigation of Forced Convection Heat Transfer in Porous Media Using Thermal Non-Equilibrium Model, International Journal of Heat and Fluid Flow*, **22**, 2001, 102-110.
14. Jiang, Pei-Xue, Si, Guang-Shu,Li, Meng, Ren, Ze-Pei, *Experimental and Numerical Investigation of Forced Convection Heat Transfer of Air in Non-sintered Porous Media*, Experimental Thermal and Fluid Sciences, **28**, 2004, 545-555.
15. Jen, Tien-Chien, Yan, T.Z., *Developing Fluid Flow and Heat Transfer in a Channel Partially Filled with Porous Medium,* International Journal of Heat and Mass Transfer, **48**, 2005, 3995-4009.
16. Jeng, Tzer-Ming, Tzeng, Sheng-Chung, Hung, Ying-Huei, *An Analytical Study of Local Thermal Equilibrium in Porous Heat Sinks Using Fin Theory*, International Journal of Heat and Mass Transfer, Article in Press, 2006.
17. Khashan, S.A., Al-Amiri, A.M., Pop, I., *Numerical Simulation of Natural Convection Heat Transfer in a Porous Cavity Heated From Below Using a Non-Darcian and Thermal Non-Equilibrium Model,* International Journal of Heat and Mass Transfer, Article in Press, 2005.
18. Manzan M., Comini, G., *Inflow and Outflow Boundary Conditions in the Finite Element Solution of the Streamfunction-Vorticity Equations*, Communications in Numerical Methods in Engineering, **11**, 1995, 33-40.
19. Metzger, T., Didierjean, S., Maillet, D., *Optimal Experimental Estimation of Thermal Dispersion Coefficients in Porous Media*, International Journal of Heat and Mass Transfer, **47**, 2004, 3341-3353.
20. Munson, Bruce R., Young, Donald F., Okiishi, Theodore H., *Fundamentals of Fluid Mechanics*, 4th Edition, John Wiley & Sons, Inc., New York, 2002.
21. Napolitano, M., Pascazio, G., Quartapelle, L., *A Review of Vorticity Conditions in the Numerical Solution of the $\zeta - \psi$ Equations*, Computers and Fluids, **28**, 1999, 139-185.
22. Nield, D.A., Kuznetsov, A.V., *Local Thermal Nonequilibrium Effects in Forced Convection in a Porous Medium Channel: A Conjugate Problem*, International Journal of Heat and Mass Transfer, **42**, 1999, 3245-3252.
23. Ochoa-Tapia, J. Alberto, Whitaker, Stephen, *Heat Transfer at the Boundary Between a Porous Medium and a Homogeneous Fluid*, International Journal of Heat and Mass Transfer, Vol 40, No 11, 1997, 2691-2707.

24. Pavel, Bogdan I., Mohamad, Abdulmajeed A., *An Experimental and Numerical Study on Heat Transfer enhancement for Gas Heat Exchangers Fitted with Porous Media*, International Journal of Heat and Mass Transfer, **47**, 2004, 4939-4952.
25. Vafai, K., Kim, S.J., *On the Limitations of the Brinkman-Forchheimer-extended Darcy Equation*, International Journal Heat and Fluid Flow, **16**, 1995, 11-15.
26. Zhang, H.Y., Huang, X.Y., *Volumetric Heat Transfer Coefficients in Solid-Fluid Porous Media; Closure Problem, Thermal Analysis and Model Improvement with Fluid Flow,* International Journal of Heat and Mass Transfer, **43**, 2000, 3417-3432.